REGIONAL GEOLOGY OF LUNAR SPINEL-RICH UNITS IN SINUS AESTUUM

L.R. Gaddis[1], J. Sunshine[2], N. Petro[3], J. Hagerty[1], J. Skinner[1] and T. Gaither[1]

[1]Astrogeology Science Center, U.S.G.S., Flagstaff, AZ (lgaddis@usgs.gov). [2]Univ. Maryland, Dept. Astronomy, College Park, MD.
[3]NASA/GSFC, Code 698, Greenbelt, MD.

Overview: The discovery of spinel-rich units in Sinus Aestuum from the Chandrayaan-1 Moon Mineralogy Mapper (M^3) instrument [1] was followed by other studies confirming the unique composition of these deposits [2, 3]. Here we describe and interpret the regional geology of the Sinus Aestuum region as a means to infer the origin and character of the widespread, spinel-rich unit.

Data: We used data from the Kaguya Terrain Camera (TC; ~10 m/pixel, [4]) and Multiband Imager (MI; 5 visible or VIS wavelength channels at 415 to 1000 nm, ~20 m/pixel [5]), the Lunar Reconnaissance Orbiter Narrow Angle (NAC; 0.5 to 2.0 m/pixel) and Wide Angle Cameras (WAC; ~100 m/pixel [6]) and the Lunar Orbiter Laser Altimeter (LOLA [7]), and GRAIL derived free-air gravity [8] and crustal thickness (model 2 [9]).

Spinel Deposits: Fe/Cr spinel-rich units are unique on the Moon and they are found only in the Sinus Aestuum (SA) region [1] in association with very dark units that mantle highland regions located to the S and SW of Sinus Aestuum [10-12] (**Figures 1-5**). Spectral signatures of spinel (primarily strong 2 µm/1 µm ratios) are observed throughout mantled highlands of SA, but the strongest signatures occur as localized concentrations associated with many of the numerous, small volcanic vents [13] mapped across SA [14, 15]. Spinel-rich pyroclastic units are observed in association with mare basalts and basaltic pyroclastic glasses and they provide information on the oxygen fugacity of the magmatic systems within which they formed and their behavior during the early stages of crystallization [16].

Regional Geology: In addition to the pyroclastic mantling deposits in SA, many small cone- (**Figure 3**) and dome-like features are observed.

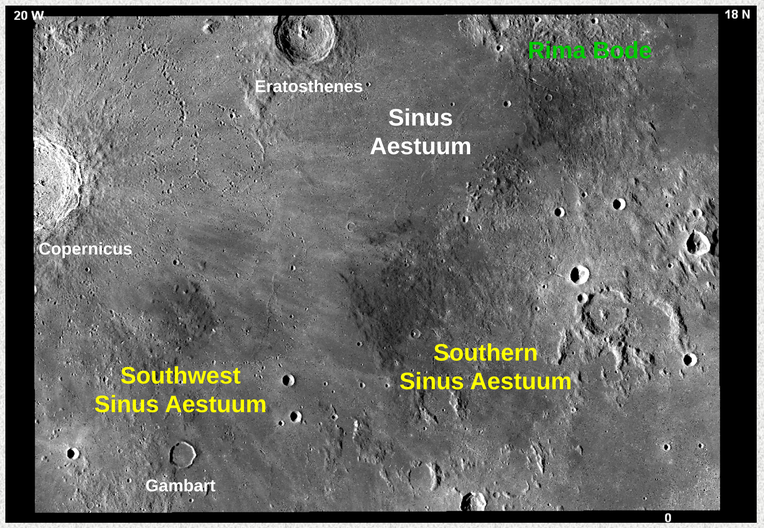

Figure 1. TC mosaic of the Sinus Aestuum and Rima Bode (SARB) region (0-18 N, 0-20 W). Dark deposits of Southern Sinus Aestuum (SSA), Southwest Sinus Aestuum (SWSA) and Rima Bode (RB) are pyroclastic in origin. Spinel-rich deposits are observed in SSA and SWSA but not RB. Eratosthenes crater is 58 km in diameter. Bright rays and secondary craters from Copernicus crater (dia. 93 km) are superimposed on SWSA and SSA deposits and maria in Sinus Aestuum.

Numerous fissures and rilles are observed in younger SA maria, but many are superimposed on and thus postdate the emplacement of the pyroclastic materials [17]. In some areas, cone-like features [13] are surrounded by dark mantles that appear to overlay localized maria north of the mantled highlands, suggesting that eruption of some of the pyroclastic material occurred after the maria.

Discussion: The geologic history of the SA region is complex and the surficial expression of the observed rocks extends back before the origin of the Imbrium basin to the north (~3.85 Ga [18]). The spinel-bearing rocks of SA appear to be co-located with deposits of the ancient Fra Mauro Formation, extending as far north as Eratosthenes crater. However, only the SA portions of the Fra Mauro Formation are spinel-bearing. The largest continuous expanses of spinel-bearing rocks are located within the darkest hummocky highlands, SE of the SA maria and SW of RB. However, not all mantled highlands in SA show spinel signatures [13, 19]. Younger maria (~2.8-3.5 Ga [16]) embay the mantled highlands, and cover, surround and embay a large population of likely localized pyroclastic vents. Occasional vents with mantle superimposed on the mare in SA suggest that this type of volcanism also occurred intermittently after mare emplacement. It appears that the regional pyroclastic mantle on the highlands in SA originated from multiple explosive eruptions, at least some of which may have been large [11].

Further work is needed to determine whether spinel-bearing exposures of SA are associated strictly with the pyroclastic deposit or whether subsurface rocks also contain spinel.

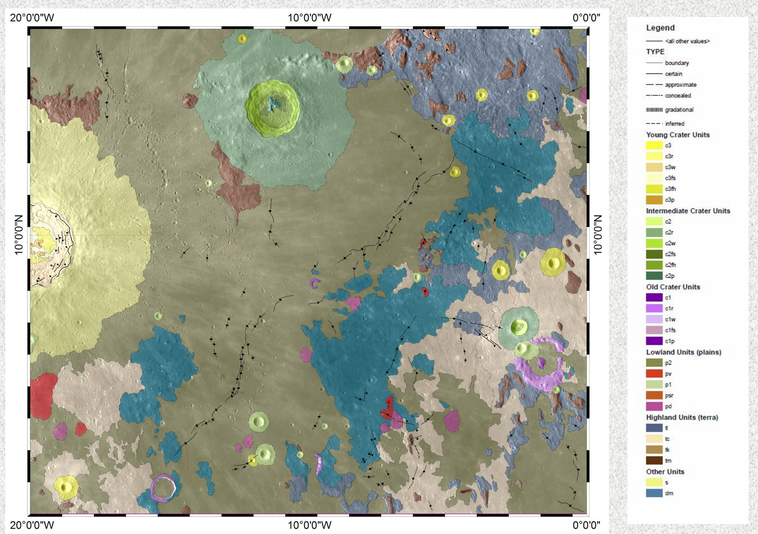

Figure 2. Preliminary updated geologic map (1:2.5M) of the Sinus Aestuum and Rima Bode regions. Mantled units (dark blue) are superimposed on ancient highlands units of the Fra Mauro Formation (buff).

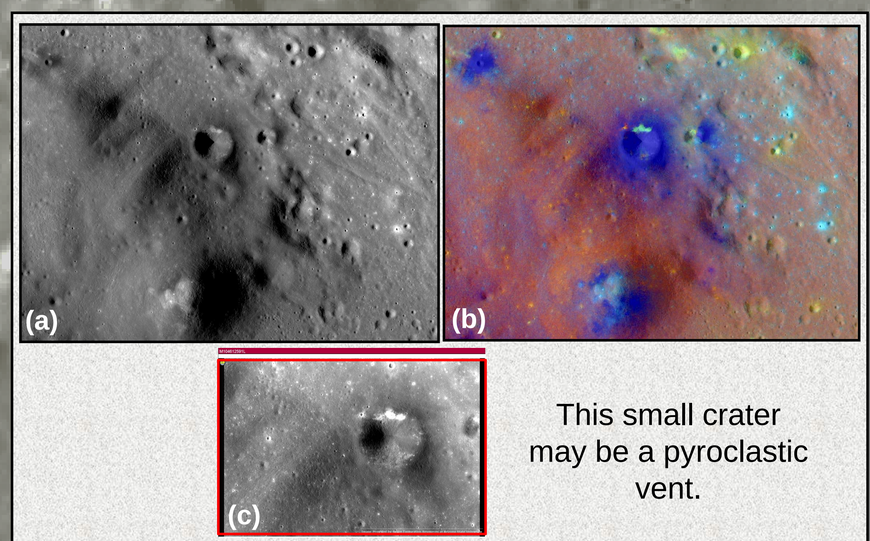

This small crater may be a pyroclastic vent.

Figure 3. Views of crater (diam. 1.5 km) in northern SWSA (red box, Figure 4). (a) TC view of crater showing dark, smooth mantle with little rubble and mantled hill to south with bald summit. (b) MI MAP view (R=750/415, B=750/950, B=415/750) showing mature pyroclastic material (red, orange) and immature pyroclastic material (blue). The crater ejecta is very limited in extent and asymmetric. (c) LROC NAC image (M104612591L, 1.2 m/p, 51° inc.) showing mantled rim. North is toward the top in each view.

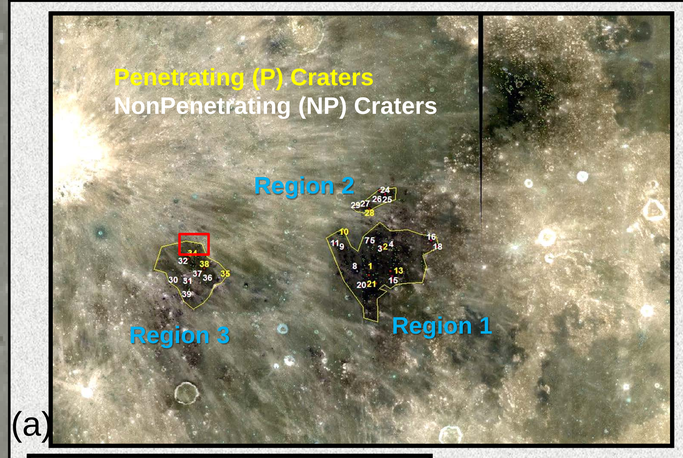

In Region 1 (SE), deposit thickness ranges from 14 m (shallowest P) to at least 36 m (deepest NP). D_{exc} for NP craters (n=11) ranges from 10 m to 36 m, and D_{exc} for P craters (n=8) ranges from 14 m to 200 m.

In Region 2 (NE), deposit thickness ranges from 12 m (shallowest P) to at least 33 m (deepest NP). D_{exc} for NP craters (n=6) ranges from 11 m to 33 m, and D_{exc} for P craters (n=1) is 12 m.

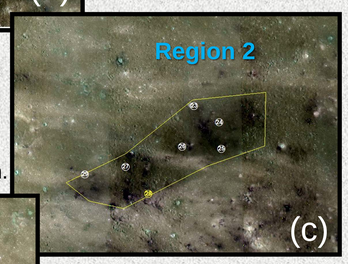

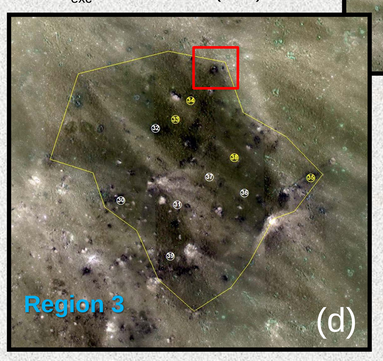

In Region 3 (W), deposit thickness ranges from 8 m (shallowest P) to at least 33 m (deepest NP). D_{exc} for NP craters (n=5) ranges from 9 m to 33 m, and D_{exc} for P craters (n=4) ranges from 8 m to 16 m.

Figure 4. (a) MI MAP views (bands 3, 2, 1 as RGB) of SARB. **(b-d)** Pyroclastic deposit thickness can be estimated using diameter measurements of penetrating (P) and non-penetrating (NP) craters and calculating depth of excavation (D_{exc}) (after [20]). Although the dark units are sparser to the W, deposits up to ~30 m deep are estimated in SARB.

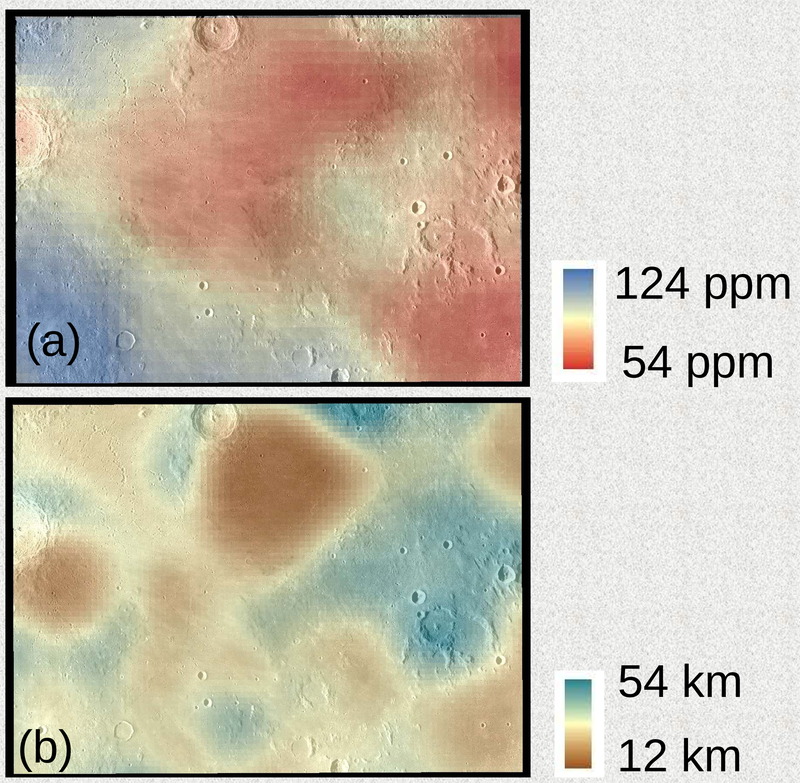

Figure 5. (a) Thorium (half-degree [21]) and (b) Crustal Thickness (Model 2 of [9]) data for the SARB region. There is an elevated radioactivity level associated with the SWSA deposits, and a relatively thin crust in the SARB region. Free-air gravity data for this area (not shown) suggest the presence of a "mascon" [22].

REFERENCES

[1] Sunshine, et al., 2010, LPS 41, abs. #1508. [2] Bhattacharya et al., 2013, LPS 43, abs. #1387; [3] Yamamoto et al., 2013, GRL 40, 4549-4554. [4] Haruyama et al., 2008, Adv. Sp. Res. 42, 310-316. [5] Ohtake et al., 2010, Space Sci. Rev. 154, 57-77. [6] Robinson et al., 2010, Space Sci. Rev. 150, 81-124. [7] Smith et al., 2010, GRL 37, L18204. [8] Zuber et al., 2013, Science, 339, 668-671. [9] Wieczorek et al., 2013, Science, 339, 671-675. [10] Head, 1974, PLPSC5, 207-222. [11] Gaddis et al., 1985, Icarus, 61, 461-489. [12] Gaddis et al., 2003, Icarus, 161 262–280. [13] Sunshine et al., *this meeting.* [14] Schmitt et al., 1967, USGS I-515 map, LAC-58. [15] Wilhelms, 1968, USGS I-548 map, LAC-59. [16] Taylor et al., 2009, AGU Fall Meeting, #P34A-07. [17] Hurwitz et al., 2013, PSS, 79-80, 1-38. [18] Wilhelms, 1987, USGS Prof. Paper 1348. [19] Weitz et al., *this meeting.* [20] Melosh, 1989, Impact Cratering, A Geologic Process, 245 pp., Oxford Press. [21] Lawrence et al., 2002, New Views of the Moon, Europe. [22] Melosh et al., 2013, Science, 340, 1552-1555.

ACKNOWLEDGMENTS

This work was funded by the NASA Planetary Geology & Geophysics program (Gaddis, Hagerty, Skinner, Gaither). We thank the Japanese (JAXA) SELENE/Kaguya TC and MI instrument teams and the mission data archive for providing some of the data used here.

USGS science for a changing world

45th LPSC, 2014
ABSTRACT #2254